AGU PUBLICATIONS

Geophysical Research Letters

RESEARCH LETTER
10.1002/2013GL058740

Key Points:
- Seasonal predictability of the AWP from state of art climate models is analyzed
- Models show promise in AWP predictability
- Models show skill in U.S. summer rainfall predictability

Correspondence to:
V. Misra,
vmisra@fsu.edu

Citation:
Misra, V., and H. Li (2014), The seasonal climate predictability of the Atlantic Warm Pool and its teleconnections, *Geophys. Res. Lett.*, *41*, doi:10.1002/2013GL058740.

Received 18 NOV 2013
Accepted 27 DEC 2013
Accepted article online 3 JAN 2014

The seasonal climate predictability of the Atlantic Warm Pool and its teleconnections

Vasubandhu Misra[1,2,3] and H. Li[1,2]

[1]Department of Earth, Ocean, and Atmospheric Science, Florida State University, Tallahassee, Florida, USA, [2]Center for Ocean-Atmospheric Prediction Studies, Florida State University, Tallahassee, Florida, USA, [3]Florida Climate Institute, Florida State University, Tallahassee, Florida, USA

Abstract Our study reveals that there is promising seasonal predictability of the Atlantic Warm Pool (AWP; defined as the area enclosed by the 28.5°C isotherm in tropical western Atlantic) and its associated teleconnections of late summer-early fall seasonal rainfall anomalies over the continental US displayed by a subset of the North American Multi-Model Ensemble (NMME). We find that of the four NMME models at least two models (CFSv2 and GFDL) exhibit consistently useful deterministic and probabilistic skill in predicting the July-October (JASO) seasonal anomalies of the area of the AWP at lead times of up to four months. These two models shown are shown to beat the observed persistence skill by a significant margin at all lead times with the exception of lead time zero. The two NMME models also skillfully predict the teleconnections of the JASO AWP anomalies with the corresponding seasonal JASO rainfall anomalies in the eastern Mississippi valley. These prediction skills are significant improvement in warm season rainfall predictability over the continental US.

1. Introduction

The Atlantic Warm Pool (AWP) has received considerable attention in the recent past with its influence on the North American climate anomalies and weather extremes [*Wang et al.*, 2006; *Wang and Lee*, 2007; *Misra et al.*, 2011]. The area of the 28.5°C isotherm in the north western tropical Atlantic Ocean defines the AWP. The area of this specific isotherm displayed the most interannual variability in the region [*Misra et al.*, 2012]. Although there is evidence to indicate that AWP is modulated at intraseasonal [*Higgins and Shi*, 2001] and decadal [*Wang et al.*, 2008] time scales as well. At the interannual scales, *Wang et al.* [2006] have shown that large (small) areas of AWP are associated with less (higher) rainfall in the mid-west region of the US and higher (lower) seasonal Atlantic tropical cyclone activity. This raises considerable interest in the prediction of the AWP at the seasonal time scales. However, our prior studies of evaluating the global coupled ocean-atmosphere models have indicated sobering results [*Misra and Chan*, 2009; *Kozar and Misra*, 2012; *Liu et al.*, 2012, 2013]. For example, *Kozar and Misra* [2012] find that in the Coupled Model Intercomparison Project Phase 5 (CMIP5) suite of models there is a pathological cold bias in the AWP region with the exception of very few models, which exhibit unrealistic eastward extension of the AWP. Similarly *Misra and Chan* [2009] showed that the seasonal prediction skill of the AWP in the Climate Forecast System version 1 [CFSv1; *Saha et al.*, 2006; the operational seasonal forecast model of the National Center for Environmental Prediction] was rather poor although seasonal cycle of the AWP was reasonably simulated by CFSv1.

The North American Multi-Model Ensemble [NMME; *Kirtman et al.*, 2013] offers a new opportunity to examine the seasonal predictability of the AWP from a new generation of global coupled ocean-atmosphere models. The NMME was motivated by a growing number of studies, which indicated that multi-model strategy was a practical approach to resolve forecast uncertainty [*Palmer et al.*, 2004, 2008; *Hagedorn et al.*, 2005]. Furthermore, the multi-institutional effort of the NMME also offers far more realizations (ensemble members) of the seasonal forecast than from a single model, which allows for robust quantitative estimates of the forecast uncertainty. The phase-I of the NMME as *Kirtman et al.* [2013] claim, is an "NMME of opportunity," as in, the contributing modeling groups used their independently developed initialization and prediction protocols for their respective hindcasts, to encourage a wider participation of the climate modeling centers. NMME was therefore considered as an "opportunity" to further seasonal predictability through multi-model approaches. Therefore, it should be remembered that differences in the seasonal hindcasts across models in phase-I of the NMME could be realized both from model differences and the initial condition differences.

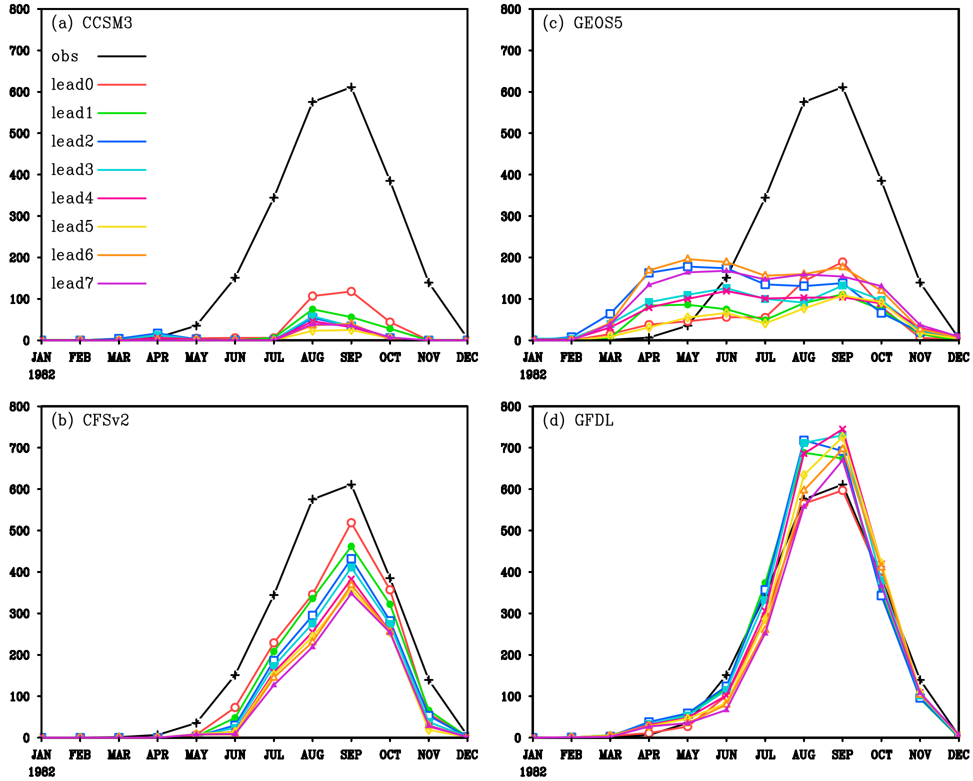

Figure 1. The climatology of the seasonal cycle of the AWP area (10^4 km^2) of the ensemble mean as a function of lead time (month) for the four NMME models overlaid with observations.

The NMME retrospective seasonal forecasts cover the period of 1982–2012. At the time of the beginning of this analysis there were four NMME models whose monthly mean forecast fields were made available from http://www.cpc.ncep.noaa.gov/products/NMME/, which are identified by their acronyms in this paper: Community Climate System Model version 3 (CCSM3), Climate Forecast System version 2 (CFSv2), Goddard Earth Observing System Model version 5 (GEOS5), and Geophysical Fluid Dynamics Laboratory Coupled Model version 2.2 (GFDL). Note that these models are currently in operational use. Since then two more from the Canadian Modeling Center have been added to the repository, which we have not analyzed in this paper. They had varying number of ensemble members but for purposes of being consistent we used six members from each as that was the least used in one of the model hindcasts. Each of these models in addition had their own methodology of generating the ensemble members, which is described in *Kirtman et al.* [2013].

In this study we will examine the climatology and the anomalies of the area of the 28.5C isotherm anomalies in the northwest tropical Atlantic Ocean predicted by the four NMME models at different lead times. In addition, we will also examine the associated teleconnection of rainfall over the continental US.

2. Results

We shall largely focus on the July–August–September–October (JASO) seasonal mean anomalies (except in Figure 1), which coincides with the seasonal peak of the AWP area. Therefore, lead 0 for JASO average would mean a start time of early July or late June, lead 1 would mean a start time of early June or late May, and so on. The most advance lead time for JASO offered by the NMME hindcast data across all models is a lead time of 4 months, which corresponds to a start time of early March or late February.

For validation of the seasonal hindcasts, we use Optimally Interpolated SST version 2 [OISSTv2; *Reynolds et al.*, 2002] for SST and Climate Prediction Center Merged Analysis of Precipitation [CMAP; *Xie and Arkin*, 1997] for rainfall. OISSTv2 and CMAP are available at 1° and 2.5° grid resolution, respectively, for the period 1982–2010 that coincides with the analysis of the NMME hindcasts in this paper.

2.1. Climatology

As mentioned earlier, the AWP has a distinct seasonal cycle with the area of the 28.5°C being climatologically largest in September (Figure 1). In Figure 1, the lead time is calculated with respect to the month in question. For example, leads 0 and 7 for month of January correspond to start times of January and June (of the previous year) of the seasonal hindcast, respectively. The GFDL model reproduces the observed seasonal cycle of the area of the AWP reasonably well. The CFSv2 exhibits a negative bias throughout the year but maintains the observed seasonal peak of the area of AWP being largest in September. However, CCSM3 and GEOS5 have a significant cold bias with the latter also exhibiting an unrealistic bi-annual peak in the seasonal cycle of the area of the AWP. In addition, we find that there is a distinct drift towards cold bias in all models, with the cold bias becoming more severe with increasing lead time. The seasonal mean errors of the area of the AWP for the JASO season (Figure 2a) of the ensemble mean clearly reiterate the negative bias. In Figure 2a, CCSM3 and GEOS5 display the most significant negative bias and GFDL model the least at all lead times.

2.2. Deterministic Skill

The correlations of the forecasted JASO seasonal mean AWP area are shown in Figure 2b from the four NMME models along with the corresponding correlations of the observed persistence of using the AWP area at the time of the start of the seasonal hindcast for a given lead time. For example, persistence with observed AWP area anomalies in March, April, May, June, and July as a forecast for the JASO seasonal mean anomalies of AWP has a correlation of 0.53, 0.49, 0.60, 0.72, and 0.80, respectively. It is quite interesting to note that the correlations of the model forecasts exceed the skill of the observed persistence at all lead times for only one model (CFSv2). In contrast, CCSM3 is poorer than observed persistence at all lead times (Figure 2b). On the other hand, GFDL performs better than observed persistence at all lead times except at lead 0, where it is marginally below the observed persistence. Similarly, GEOS5 is superior (inferior) to the correlations displayed by the observed persistence at leads 2, 3, and 4 (leads 1 and 0). It may also be noted that the degradation in the correlation with the lead time is modest in all four models relative to the skill of the observed persistence.

If we examine the ratio of the ensemble mean to the ensemble spread as a measure of signal-to-noise ratio as a function of lead time (Figure 2c), we observe that the CCSM3 has the least signal-to-noise ratio component at all lead times followed by GEOS5 (Figure 2c). GFDL and CFSv2 show a consistent decline of the signal-to-noise ratio with lead time unlike GEOS5 and CCSM3 (Figure 2c). This behavior is consistent with the increase (decrease) in ensemble spread in GFDL and CFSv2 (GEOS5 and CCSM3) in Figure 2d. The diagnosis in Figures 2c and 2d show a clear divide between the two pairs of models CFSv2 and GFDL from CCSM3 and GEOS5. It is apparent from the given significant negative bias in the AWP area in CCSM3 and GEOS5 (Figure 1) that the signal-to-noise ratio is comparatively small as the anomalies are small. Furthermore, the climate drift in these two models is so severe that the ensemble spread reduces with increasing lead time of the seasonal hindcast. Figure 2d shows that at a lead of 1 month the ensemble spread is the least in the GFDL and in the CFSv2 models. Thereafter, there is a general tendency for the spread to increase with lead time in both these models. This is likely reflective of the fact that NMME protocol did not call for using initial conditions for all models. As a result, the spread is slightly higher at initial time, which subsides after some adjustment within a month and then begins to increase again owing to chaotic nature of the non-linear system.

2.3. Probabilistic Skill

In Figure 3, we show the Area under the Relative Operating characteristic Curve (AROC) as a measure of the probabilistic skill score for high, medium, and low tercile anomalies of the area of the AWP. Owing to significant negative bias in CCSM3, it displays some useful skill (that exceeds climatology) (In order for AROC to be skillful in a model, it should exceed a value of 0.5. Otherwise, it is considered to be on par or below the value of climatology.) only for high tercile events while there is no useful skill for the low and middle tercile events of anomalous area of the AWP (Figure 3a). In all the other models there is significant probabilistic skill to be harvested at all lead times for the high and medium terciles. However, for the low tercile AWP events the models are not consistent in showing a superior skill than climatology. For example, CFSv2 (Figure 3b) and GFDL (Figure 3d) display AROC dropping below 0.5 at 4 month and 3 month leads. While GEOS5 intriguingly has AROC above 0.5 at all leads for all tercile events of the area of the AWP. To examine if this was a reflection of the limited number of ensemble members, we compared the AROC values from all available 24 members (Figure 3f) of the CFSv2 hindcasts with using only 10 ensemble members (Figure 3e). The figure clearly shows that the changes in the AROC are rather insignificant for all terciles. In other words, Figures 3e

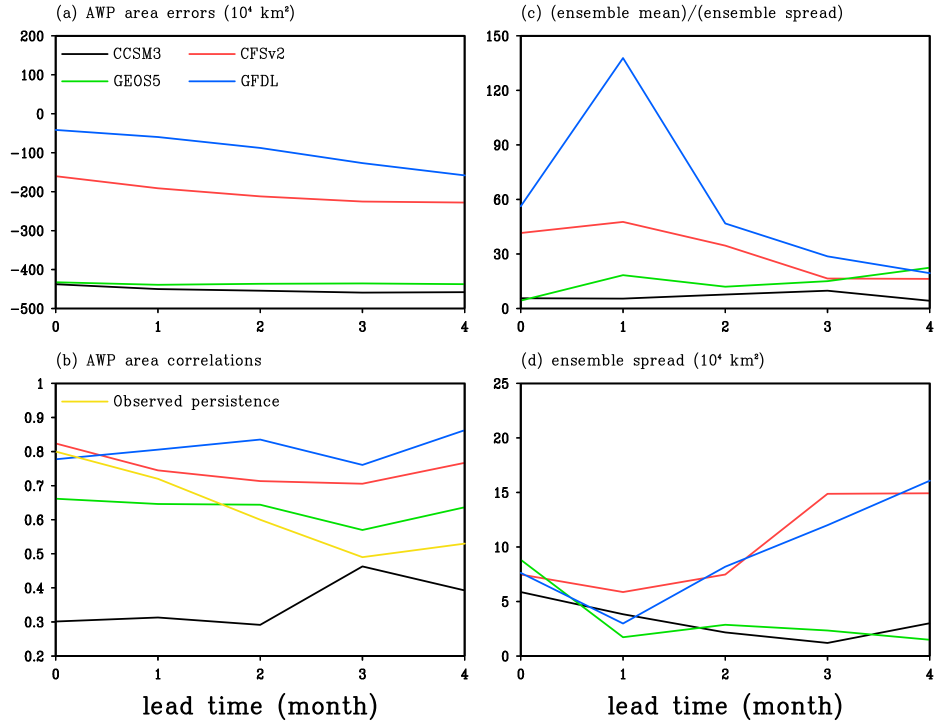

Figure 2. The seasonal mean Jul–Aug–Sep–Oct (JASO) (a) errors of the Area of AWP (10^4 km^2), (b) correlation, (c) the ratio of ensemble mean to ensemble spread of the mean JASO area of AWP, and (d) the ensemble spread of the mean JASO AWP area (10^4 km^2), as a function of lead time (month) for CCSM3, CFSv2, GEOS5, and GFDL. In Figure 2b, correlations of the observed persistence are also shown. Leads 0, 1, 2, 3, and 4 are July, June, May, April, and March starts, respectively.

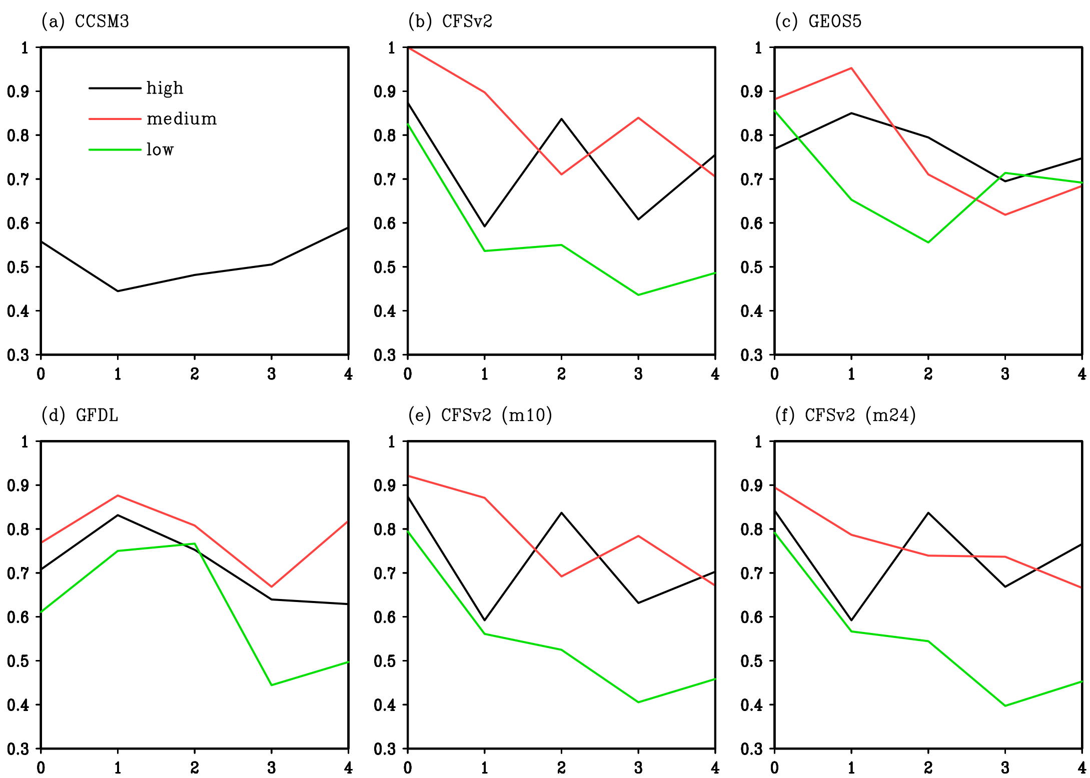

Figure 3. The area under the relative operating characteristic curve for the seasonal mean prediction of the mean JASO area of the AWP from the NMME models (six ensembles) of (a) CCSM3, (b) CFSv2, (c) GEOS5, and (d) GFDL as a function of lead time of the forecast. Figures 3e and 3f are same as Figure 3b but for CFSv2 with 10 and 24 ensemble members.

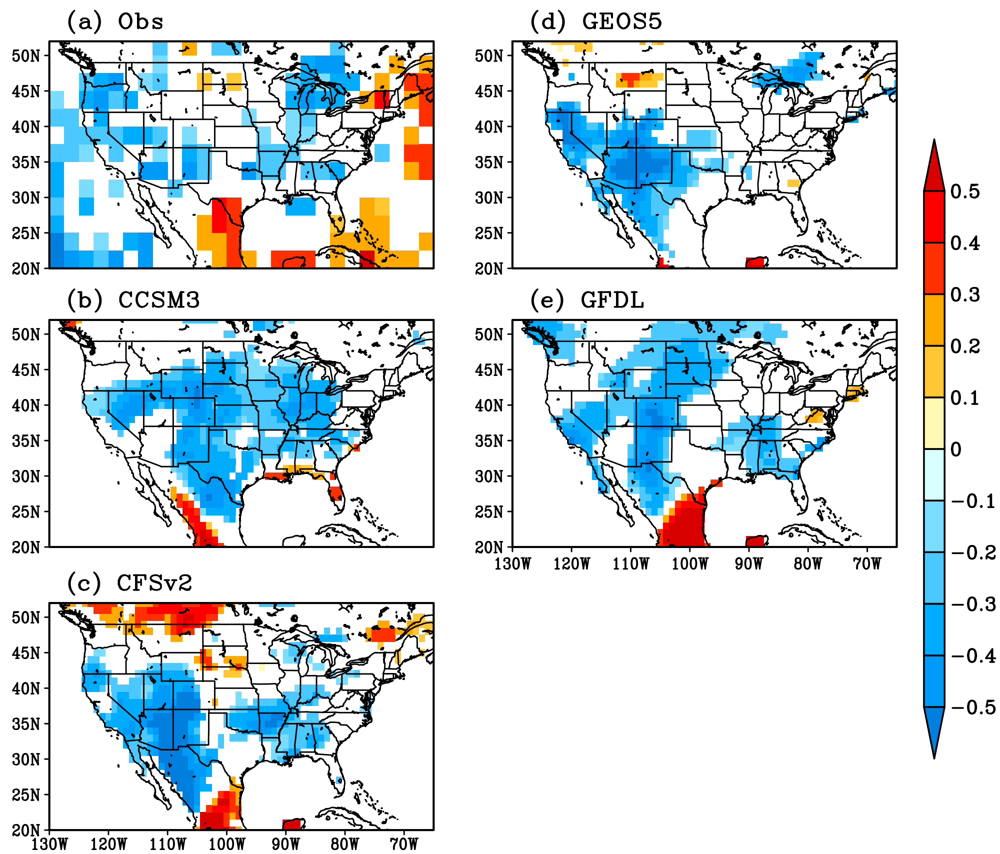

Figure 4. The contemporaneous correlation of JASO seasonal anomalies area of the AWP with the corresponding seasonal precipitation anomaly from (a) observation, (b) CCSM3, (c) CFSv2, (d) GEOS5, and (e) GFDL.

and 3f suggest that the limitation of a small number of ensemble members in the NMME may not necessarily reflect a bias in the skill scores in regard to the AWP area anomalies.

2.4. Teleconnections

The reason the AWP anomalies are of interest is because it forces a contemporaneous seasonal rainfall anomaly over a significant area of North America besides influencing Atlantic seasonal tropical cyclone activity [*Wang et al*., 2006]. In Figure 4a, we show the contemporaneous correlation of the observed JASO seasonal anomalies area of the AWP with the corresponding seasonal precipitation anomaly. It is seen in Figure 4a, consistent with previous studies, that the weaker (stronger) JASO seasonal precipitation anomalies in eastern Mississippi valley are associated with large (small) AWP. It is noteworthy that with the exception of the GEOS5, all other models are able to pick this teleconnection reasonably well. However, CCSM3 unlike observations show nearly the entire continental US JASO mean precipitation anomalies showing a strong relationship with AWP anomalies. Similarly, CFSv2 and GFDL show erroneously significant modulation of precipitation in southwestern United States in addition to that over eastern Mississippi valley. Furthermore, unlike observations the rainfall anomalies do not extend to the northeast part of the Mississippi valley in the GFDL hindcasts.

3. Conclusions

In this paper we have examined the seasonal predictability of the AWP seasonal anomalies of its area on the sea surface and its associated teleconnection with the late summer-early fall rainfall over the continental US from the NMME models. The NMME models are a co-ordinated set of dynamical seasonal predictions involving six different coupled ocean-atmosphere models, which have been initialized independent of each other. The NMME presents an exhaustive set of retrospective seasonal hindcasts that covers the period from 1982 to present, with a minimum of six ensemble members per model and initialized at the beginning of every month of the year and integrated out to a minimum of 9 months. NMME represents the state of the art in global seasonal prediction.

We show that there is promising seasonal prediction skill in predicting JASO seasonal mean AWP area anomalies at all leads ranging from zero month to four month lead in at least CFSv2 and GFDL models. CCSM3 and GEOS5 exhibit a grave negative bias in the seasonal cycle of the AWP area, which reflects quite clearly in the deterministic skill of the model. However, the probabilistic skill analysis of the AWP area seems to obfuscate this systematic error especially in GEOS5. In addition, these models (e.g., CFSv2 and GFDL) also display useful skill in the associated teleconnections of the JASO area anomalies of the AWP with JASO seasonal rainfall anomaly over the eastern Mississippi valley. These results displayed by the two NMME models mark a significant progress from our earlier study on seasonal predictability of the AWP [*Misra and Chan*, 2009], which disappointingly did not exhibit any useful probabilistic skill at any lead time of the seasonal forecast from CFSv1. However, these set of hindcasts seem to set a high standard in terms of AWP predictions and warm season rainfall predictability over the continental US for future improvements.

Acknowledgments
This work was supported by grants from NOAA (NA12OAR4310078, NA10OAR4310215, NA11OAR4310110), and USDA (2010-38890-20734).

The Editor thanks two anonymous reviewers for assistance evaluating this manuscript.

References

Hagedorn, R., F. J. Doblas-Reyes, and T. N. Palmer (2005), The rationale 546 behind the success of multi model ensembles in seasonal forecasting - I. Basic concept, *Tellus Ser. A*, *57*, 219–233, doi:10.1111/j.1600-0870.2005.00103.x.

Higgins, W., and W. Shi (2001), Intercomparison of the principal modes of interannual and intraseasonal variability of the North American monsoon system, *J. Clim.*, *14*, 403–417.

Kirtman, B. P., et al. (2013), The North American Multi-1 Model Ensemble (NMME): Phase-1 Seasonal to Interannual Prediction, Phase-2 Toward Developing Intra-Seasonal Prediction, *Bull. Am. Meteorol. Soc.*, doi:10.1175/BAMS-D-12-00050.1, in press.

Kozar, M., and V. Misra (2012), Evaluation of Twentieth-Century Atlantic Warm Pool Simulations in Historical CMIP5 Runs, *Clim. Dyn.*, doi:10.1007/s00382-012-1604-9.

Liu, H., C. Wang, S.-K. Lee, and D. B. Enfield (2012), Atlantic warm pool variability in the IPCC twentieth-century climate simulations, *J. Clim.*, *25*, 5612–5628, doi:10.1175/JCLI-D-11-00376.1.

Liu, H., C. Wang, S.-K. Lee, and D. B. Enfield (2013), Atlantic warm pool variability in the CMIP5 simulations, *J. Clim.*, *26*, 5315–5336, doi:10.1175/JCLI-D-12-00556.1.

Misra, V., and S. Chan (2009), Seasonal Predictability of the Atlantic Warm Pool in the NCEP CFS, *Geophys. Res. Lett.*, *36*, L16708, doi:10.1029/2009GL039762.

Misra, V., L. Moeller, L. Stefanova, S. Chan, J. J. O'Brien, T. J. Smith III, and N. Plant (2011), The influence of the Atlantic Warm Pool on Florida Pan handle Florida Sea Breeze, *J. Geophys. Res.*, *116*, D00Q02, doi:10.1029/2010JD015260.

Misra, V., A. Stroman, and S. DiNapoli (2012), The rendition of the Atlantic warm pool in the reanalyses, *Clim. Dyn.*, doi:10.1007/s00382-012-1474-1.

Palmer, T. N., et al. (2004), Development of a European multi-model ensemble system for seasonal-to-interannual prediction (DEMETER), *Bull. Am. Meteorol. Soc.*, *85*, 853–872.

Palmer, T. N., F. J. Doblas-Reyes, A. Weisheimer, and M. J. Rodwell (2008), Toward seamless prediction: Calibration of climate change projections using seasonal forecast, *Bull. Am. Meteorol. Soc.*, *89*, 459–470.

Reynolds, R. W., N. A. Rayner, T. M. Smith, D. C. Stokes, and W. Wang (2002), An improved in situ and satellite SST analysis for Climate, *J. Clim.*, *15*, 1609–1625.

Saha, S., et al. (2006), The NCEP Climate Forecast System, *J. Clim.*, *19*, 3483–3517, doi:10.1175/JCLI3812.1.

Wang, C., and S.-K. Lee (2007), Atlantic warm pool, Caribbean low-level jet, and their potential impact on Atlantic hurricanes, *Geophys. Res. Lett.*, *34*, L02703, doi:10.1029/2006GL028579.

Wang, C., D. B. Enfield, S.-K. Lee, and C. Landsea (2006), Influences of the Atlantic warm pool on Western Hemisphere summer rainfall and Atlantic hurricanes, *J. Clim.*, *19*, 3011–3028.

Wang, C., S.-K. Lee, and D. B. Enfield (2008), Atlantic warm pool acting as a link between Atlantic multidecadal oscillation and Atlantic tropical cyclone activity, *Geochem. Geophys. Geosyst.*, *9*, Q05V03, doi:10.1029/2007GC001809.

Xie, P., and P. A. Arkin (1997), Global precipitation: A 17-year monthly analysis based on gauge observations, satellite estimates, and numerical model outputs, *Bull. Amer. Meteor. Soc.*, *78*, 2539–2558.